DYNAMIC CHANGES AND IMPACT FACTORS OF VEGETATION COVERAGE IN THE HIGHLY URBANIZED CITY: A CASE STUDY OF BEIJING, CHINA

YUAN, R. C.[1] – WANG, Z. C.[1,2*] – HU, W. M.[1,3] – YIN, C. X.[1]

[1]*Central South University of Forestry and Technology, Changsha, 410004 Hunan, China*

[2]*Key Laboratory of Soil and Water Conservation and Desertification Combating, Central South University of Forestry and Technology, Changsha, 410004 Hunan, China*

[3]*Institute of Forest Resource Information Techniques, Chinese Academy of Forestry, 100089 Beijing, China*

**Corresponding author*
e-mail: wzc366@163.com

(Received 10th Mar 2022; accepted 11th Jul 2022)

Abstract. Vegetation coverage (VC) is usually used to judge the growth status of plants and monitor the quality of the ecological environment. To better understand the dynamics and processes of VC change in urbanized cities, this research studied the impact of common natural and human factors on VC in Beijing, China from 2000 to 2015. The results showed that in Beijing, China, VC decreased by 0.1534% per year from 2000 to 2015. VC was low at an altitude range of -129~200 m and a slope range of 5~10°. Temperature and precipitation had positive effects on VC. The urban area of Beijing accounted for 40.92% of the total area. Urbanization represented by the brightness of night light had a negative impact on VC. The negative correlation between urbanization and the VC was observed mainly in the most urbanized area. From 2000 to 2015, the area of construction land increased by 1784 km^2. Between 2000 and 2015, the land use changing from waters to grassland increased the VC by 24.72%, and the land use changing from farmland to construction land decreased the VC by 17.82%. This research can provide scientific support for local policy-making to improve the urban ecological environment.
Keywords: *night time light data, urbanization, land use, correlation analysis, dimidiate pixel model*

Introduction

Urbanization has caused substantial environmental issues and threatened human health. Although the existing science and technology have made great achievements in monitoring the emission of single harmful substances, such as $PM_{2.5}$, SO_2 and NO, the comprehensive monitoring of the ecological environment is still a difficult problem. Vegetation, as the producer, is an essential part of the ecosystem. It can produce oxygen and organic matter through photosynthesis and provide animals with a stable living environment (Pan et al., 2017). Vegetation coverage (VC) is often used to judge the growth status of plants and monitor the quality of the ecological environment (Song et al., 2017). It usually refers to the vertical projection area of aboveground vegetation organs to the study area. The influencing factors of VC include human activities and natural factors. Natural factors include slope, altitude, temperature, and precipitation (Liao et al., 2014; Rezaei and Gurdak, 2020). Different natural conditions lead to different soil water, fertility and enzyme activities, which affect the growth of vegetation. Human factors include deforestation, overgrazing, and urban construction (Hao et al., 2020). In recent years, the population and economy have shown explosive growth because of the development of science and technology. It means that human demand for natural

http://www.aloki.hu ● ISSN 1589 1623 (Print) ● ISSN 1785 0037 (Online)
DOI: http://dx.doi.org/10.15666/aeer/2006_48194834

resources expands continually, and it also causes a lot of damage to vegetation. Meanwhile, some human activities also positively impact VC, such as urban greening, forest protection, and nature reserve construction (Zhou et al., 2019; Janeczko et al., 2019). Remote sensing technology is an important means to monitor VC, and it can quickly carry out a large area and long-time sequence of environmental monitoring. In the field of remote sensing application, the vegetation index has been widely used to evaluate vegetation cover and its growth vitality (Wang et al., 2020b; Sharifi, 2020). Green vegetation shows different reflectance in different bands. The purpose of establishing a vegetation index is to effectively synthesize relevant spectral signals, enhance vegetation information and reduce non-vegetation information (Gao et al., 2020).

Temperature and precipitation affect vegetation diversely at different times and regions (Xia et al., 2018). At the start of the growing season, the temperature is the most important climatic element affecting most plant kinds on the Tibetan Plateau, and precipitation has a significant impact on the temperate desert, temperate steppe, and temperate desert steppe near the conclusion of the growing season. Furthermore, temperature significantly impacts the alpine steppe, alpine desert, alpine meadow, and sparse alpine vegetation (Cai et al., 2021). In the Subtropical region of China, the average annual lowest temperature and yearly precipitation showed beneficial effects on VC in more than half of all pixels. In contrast, the average annual maximum temperature had negative effects. The effect of climate change on VC was clearly heterogeneous, with the average annual lowest temperature being the primary factor (Liu et al., 2021). In the Amur River Basin, the growth season, spring, and summer had the most significant rise in grassland VC, whereas fall saw the greatest shift in forest VC. In the spring, VC is associated positively with air temperature, particularly in grassland, and negatively with precipitation, particularly in woodland (Yang et al., 2020). In the coastal wetlands of China, the majority of the annual mean vegetation coverage was lower but improved near the sea, with the opposite findings observed near land (Hao et al., 2020). In the Sichuan Province of China, the proportion of regions where relative humidity and precipitation were important drivers of VC changes was much higher than the proportion of regions where air temperature and other co-drivers were the driving forces (Li et al., 2020). In the Yangtze River Delta, the temperature has a more significant influence on plant growth than precipitation at both the yearly and monthly timeframes. Furthermore, plant growth displayed a time lag effect in response to precipitation for 1 or 2 months, but there were no such phenomena with temperature (Yuan et al., 2019).

Human factors generally have the most significant impact on VC. As the most concentrated part of human activities, cities, and towns have the most drastic changes in VC. In Otindag Sandy Land, population pressure, urbanization, industry, pastoral producing activities, and inhabitants' lifestyles had a detrimental influence on human causes. On the other hand, ecological restoration policies helped resolve the conflict between human development and vegetation degradation (Wang et al., 2020a). In China-Myanmar economic corridor, human activities including afforestation, agriculture, and building substantially impacted VC changes, and VC fluctuated a lot in the short term (Li et al., 2021). In Beijing, positive VC changes were mainly in the urban core functional regions within the Fifth Ring Road and the northern and western mountainous areas. Negative VC changes were focused from the 5th Ring Road to the 6th Ring Road's outside regions (Zhao et al., 2021). In Pearl River Delta between 2000 and 2012, the pace of urbanization grew by 0.58 per year. Urbanization enhanced vegetation covering, according to the partial correlation (Wang et al., 2021). In the Beijing–Tianjin–Hebei

http://www.aloki.hu ● ISSN 1589 1623 (Print) ● ISSN 1785 0037 (Online)
DOI: http://dx.doi.org/10.15666/aeer/2006_48194834

(BTH) region, the VC increased in minor places like Cangzhou and the Taihang Mountains but decreased in megacities like Beijing. The intensity of urbanization dropped as one moved from the urban center to the periphery, but the rate of urbanization rose (Zhou et al., 2019). In Erechim, during the research period, the vegetation area at the urban perimeter decreased by 229.98 hectares because of growing urbanization. The growth of urban regions diminished vegetation fragments. It effectively contributed to the disorderly habitation of the city, resulting in severe consequences on the environment and the local population's quality of life (Brandalise et al., 2019).

In previous studies, researchers usually used two methods to study the impact of human activities on VC. One is to eliminate the influence of natural factors on VC through residual analysis to obtain the effect of human factors on VC. Because there are too many biological factors affecting VC, it is not easy to eliminate all of them. This leads to the influence of human factors on VC being exaggerated. The second is to evaluate human activities through the whole region's GDP, population, and industrial structure. These data cannot be rasterized and correspond to the pixels of remote sensing images one by one, so the error is significant. For these problems, nighttime light data can solve them well when studying urban expansion (Liang et al., 2020; Hu and Huang, 2019). Therefore, this research used the brightness of nighttime light to represent urbanization and combines the land use, climate and topographic data of the study area to clarify the impact of these factors on VC, so as to provide a basis for local environmental protection policy-making.

Materials and methods

Site description

The site description Beijing is the capital of China (115.7°E–117.4°E, 39.4°W–41.6°W), Globalization and World Cities Study Group and Network defined Beijing as an alpha level, which means this city has a leading role and driving ability in global activities. The city governs 16 districts with a total area of 16410 km^2, and the permanent resident population in the urban area exceeds 18 million. The terrain is high in the northwest and low in the southeast; the average altitude is 43.5 m. Beijing is surrounded by mountains in the west, north and northeast, and a plain in the southeast. Beijing has a warm temperate semi-humid and semi-arid monsoon climate: The summer is hot and rainy, the winter is cold and dry, and the spring and autumn are short. 80% of the annual precipitation is concentrated in June, July and August, the average annual precipitation is about 500 mm.

Data sources

This research mainly used MOD13Q1 data, land use data, 1-km monthly mean temperature dataset for China, 1-km monthly precipitation dataset for China, ASTER GDEM and NPP-VIIRS-like nighttime light data. MOD13Q1 data was provided by NASA (https://ladsweb.modaps.eosdis.nasa.gov/), its spatial resolution is 250 m, and its temporal resolution is 16 days. MOD13Q1 includes multiple vegetation indexes, in this paper, Normalized Difference Vegetation Index (NDVI) was the only one that this research used. By downloading MOD13Q1 of Beijing from 2000 to 2015, and using MODIS Reprojection Tool to extract NDVI from the data, the spatial resolution was resampled to 30 m and the coordinate system was projected to Krasovsky_1940_Albers.

http://www.aloki.hu ● ISSN 1589 1623 (Print) ● ISSN 1785 0037 (Online)
DOI: http://dx.doi.org/10.15666/aeer/2006_48194834

And the maximum value composite method was used to synthesize data into annual maximum NDVI in ArcGIS 10.6 version, this method can eliminate the influence of aerosols and clouds on remote sensing images. Land use data of Beijing in 2000 and 2015 was provided by Geographical Information Monitoring Cloud Platform (http://www.dsac.cn/), its spatial resolution is 30 m, and it divides land use into cultivated land, forest land, grassland, water area, construction land and unused land. 1-km monthly mean temperature dataset and 1-km monthly precipitation dataset were provided by National Tibetan Plateau Data Center (http://data.tpdc.ac.cn/), the data were verified by 496 independent meteorological observation points and the results are reliable. Then this research averaged the monthly data to get the annual average precipitation and temperature of Beijing. NPP-VIIRS-like nighttime light data (https://doi.org/10.7910/DVN/YGIVCD) were used to present the urbanization level, the data used an auto-encoder model including convolutional neural networks to integrate DMSP-OLS and NPP-VIIRS nighttime light data, and the accuracy evaluation, spatial pattern, and temporal consistency are reliable. ASTER GDEM was provided by Geospatial Data Cloud (http://www.gscloud.cn/), it is a kind of Digital Elevation Model, its spatial resolution is 30 m, it was used to present altitude, and the slopes of Beijing were calculated by slope analysis tool in ArcGIS. Besides, all raster images were projected to Krasovsky_1940_Albers coordinate system and the spatial resolution was resampled to 30 m.

Methods

Dimidiate pixel model

Dimidiate pixel model (Leprieur et al., 1994; Zribi et al., 2003) is a simple and applicable method to calculate VC, according to this model, the information S observed by the remote sensing sensor can be expressed as the information S_v contributed by the vegetation part and the information S_n contributed by the non-vegetation part, the equation is:

$$S = S_v + S_n \quad \text{(Eq.1)}$$

If the VC of a pixel is assumed to be F, then the area proportion without vegetation part is $1-F$. And if the remote sensing information of the pure pixel fully covered by vegetation is S_{veg}, then the information S_v contributed by the vegetation part of the mixed pixel can be expressed as:

$$S_v = F \times S_{veg} \quad \text{(Eq.2)}$$

In a similar way, if the remote sensing information of the pure pixel fully covered by the non-vegetation part is S_{veg}, then the information S_n can be expressed as:

$$S_n = (1-F) \times S_{neg} \quad \text{(Eq.3)}$$

Now, S_v can be expressed as:

$$S = F \times S_{veg} + (1-F) \times S_{neg} \quad \text{(Eq.4)}$$

http://www.aloki.hu ● ISSN 1589 1623 (Print) ● ISSN 1785 0037 (Online)
DOI: http://dx.doi.org/10.15666/aeer/2006_48194834

After a concise mathematical manipulation, F can be expressed as:

$$F = \frac{S - S_{neg}}{S_{veg} - S_{neg}} \quad \text{(Eq.5)}$$

If NDVI was used to present the information *S*, then *Equation 5* can be expressed as:

$$F = \frac{NDVI - NDVI_{neg}}{NDVI_{veg} - NDVI_{neg}} \quad \text{(Eq.6)}$$

where *NDVI* is the NDVI value of a pixel, $NDVI_{veg}$ is the NDVI value of a pure pixel fully covered by vegetation, and $NDVI_{neg}$ is the NDVI value of a pure pixel fully covered by non-vegetation part.

The calculation of VC often needs to select an appropriate confidence level, and the value range is generally 0.5% to 5% (Zeng et al., 2003; Wu et al., 2014), according to the actual situation of the study area, it is 1% in this research. It means that if we rank the values of NDVI from small to large, the value with a cumulative percentage of 1% is $NDVI_{neg}$ and the value with a cumulative percentage of 99% is $NDVI_{veg}$.

Mann-Kendall method

The Mann-Kendall method (Benjankar et al., 2012; Martínez et al., 2011) is often used to analyze the changing trend of VC. It is a nonparametric statistical test method; its advantage is that it does not need the samples to follow a certain distribution and it is not disturbed by a few outliers. For time series X, the statistics of Mann-Kendall trend test are defined as:

$$S = \sum_{i=1}^{n-1} \sum_{j=i+1}^{n} \mathrm{sgn}(x_j - x_i) \quad \text{(Eq.7)}$$

where x_j is the ith data value of the time series, n is the length of data sample, and sgn is the symbolic function, sgn is defined as:

$$\mathrm{sgn}(\theta) = \begin{cases} 1 & \theta > 0 \\ 0 & \theta = 0 \\ -1 & \theta < 0 \end{cases} \quad \text{(Eq.8)}$$

Mann and Kendall proved that the statistics *S* obeys the normal distribution, and its mean value is 0 and the variance *Var*(*S*) is:

$$Var(S) = \frac{n(n-1)(2n+5) - \sum_{i=1}^{n} t_i (i-1)(2i+5)}{18} \quad \text{(Eq.9)}$$

where t_i is the number of ith data.

http://www.aloki.hu ● ISSN 1589 1623 (Print) ● ISSN 1785 0037 (Online)
DOI: http://dx.doi.org/10.15666/aeer/2006_48194834

The calculation equation of standardized statistics is:

$$Z_c = \begin{cases} \frac{S-1}{Var(S)} & S > 0 \\ 0 & S = 0 \\ \frac{S+1}{Var(S)} & S < 0 \end{cases} \quad \text{(Eq.10)}$$

where Z_c obeys normal distribution.

The measure of trend size is β, and the equation is:

$$\beta = Median(\frac{x_i - x_j}{i - j}) \quad \text{(Eq.11)}$$

where $1 < j < i < n$, $\beta > 0$ means an upward trend, and $\beta < 0$ means a downward trend.

The method of Mann-Kendall trend test is: null hypothesis $H_0 : \beta = 0$, when $|Z_c| > Z_{1-\alpha/2}$, the null hypothesis is rejected. And $Z_{1-\alpha/2}$ is standard normal distribution and α is significance test level. $|Z_c|$ is defined as:

$$|Z_c| \geq \begin{cases} 1.28 & \alpha = 0.1 \\ 1.64 & \alpha = 0.05 \\ 2.32 & \alpha = 0.01 \end{cases} \quad \text{(Eq.12)}$$

Correlation analysis

Correlation analysis was conducted between human activities, natural factors and VC. The calculation of the correlation coefficient is:

$$r_{xy} = \frac{\sum_{i=1}^{n}(x_i - \bar{x})(y_i - \bar{y})}{\sqrt{\sum_{i=1}^{n}(x_i - \bar{x})^2}\sqrt{\sum_{i=1}^{n}(y_i - \bar{y})^2}} \quad \text{(Eq.13)}$$

where r_{xy} is the correlation coefficient between x and y, n is the number of years, $\bar{x}$ and $\bar{y}$ are the average value of x and y, respectively.

The value of correlation coefficient is between -1 and 1. If $r_{xy} > 0$, it means there is a positive correlation between these two elements, and if $r_{xy} < 0$, it means there is a negative correlation between them. Usually, we need to conduct a test on the correlation coefficient to understand the significance of this correlation, it was done by consulting the critical value table. All significance tests of the correlation coefficients in this paper are at the confidence level α=0.05, it means a significant

http://www.aloki.hu ● ISSN 1589 1623 (Print) ● ISSN 1785 0037 (Online)
DOI: http://dx.doi.org/10.15666/aeer/2006_48194834

negative correlation when correlation coefficient $r_{xy} < -0.4973$, and it means an insignificant negative correlation when $-0.4973 \le r_{xy} < 0$. Similarly, $r_{xy} > 0.4973$ means a significant positive correlation and $0.4973 \ge r_{xy} > 0$ means an insignificant positive correlation.

Results

Spatial distribution and dynamic changes of VC

The spatial distribution of average annual VC (*Fig. 1a*) indicated that the VC in the north of Beijing is higher than the VC in the south, and the VC in the west is higher than the VC in the east. The changing trend of VC is shown in *Figure1b*, the average change trend of VC is -0.1534%/year. The VC decreased significantly in 19.33% of the study area and decreased insignificantly in 31.59% of the study area. The VC increased significantly in 13.78% of the study area and increased insignificantly in 35.30% of the study area. The increase of VC was mainly in the north and southwest of Beijing, and the decrease of VC was mainly in the south and middle of Beijing. According to statistical analysis, the average annual VC in 2001 was the highest (75.09%) and it was lowest in 2014 (68.86%). And the average annual VC of the study area between 2000 and 2015 was 72.39%.

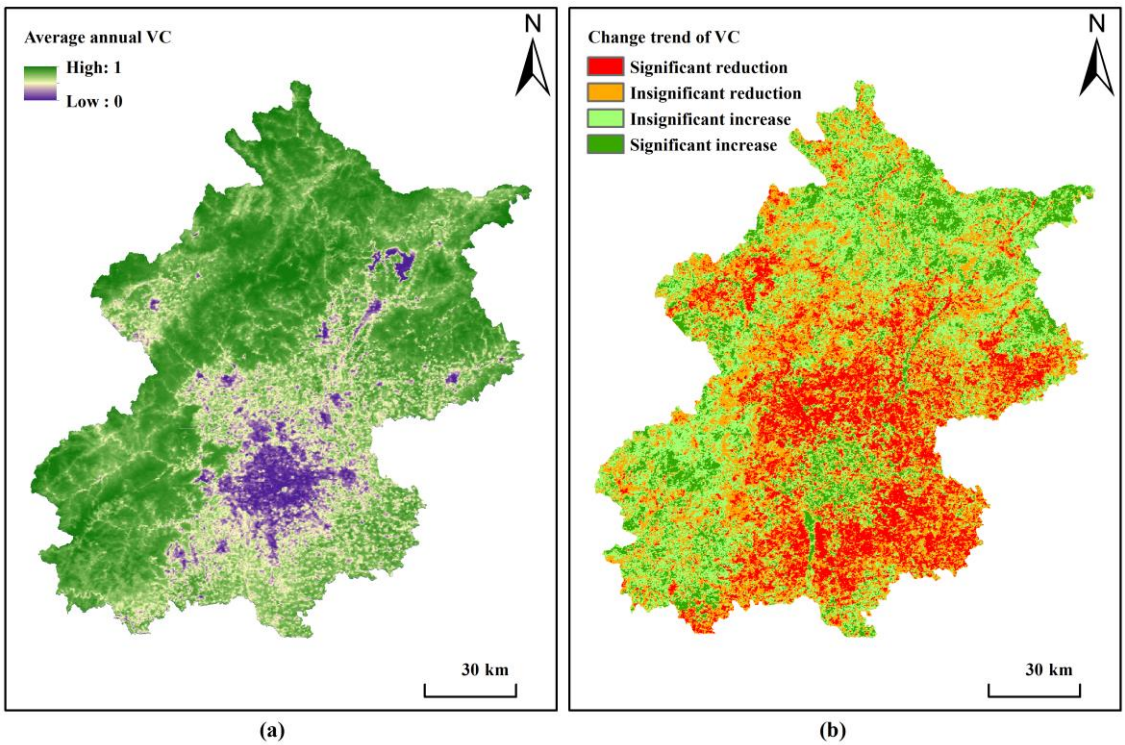

Figure 1. *Spatial distribution (a) and change trend (b) of VC in Beijing from 2000 to 2015. The significance level* α=0.05*, so when* $Z_c \le -1.64$*, the change trend is a significant reduction. When* $-1.64 < Z_c < 0$*, the change trend is an insignificant reduction. When* $Z_c \ge 1.64$*, the change trend is a significant increase, and when* $0 < Z_c < 1.64$*, the change trend is an insignificant increase*

http://www.aloki.hu ● ISSN 1589 1623 (Print) ● ISSN 1785 0037 (Online)
DOI: http://dx.doi.org/10.15666/aeer/2006_48194834

The effect of topographical factors on VC

The spatial distribution of altitude and slope in the study area is shown in *Figure 2a* and *b*, respectively. The highest altitude is 2287 m and the lowest is -129 m, and the altitude is higher in the southwest and northwest, and it is lower in the east and southeast parts. The highest slope is 78° and the lowest is 0°, and the spatial distribution of slope is basically the same as the spatial distribution of altitude. As shown in *Figure 3*, the VC showed a trend of increasing followed by decreasing at different altitudes or slopes.

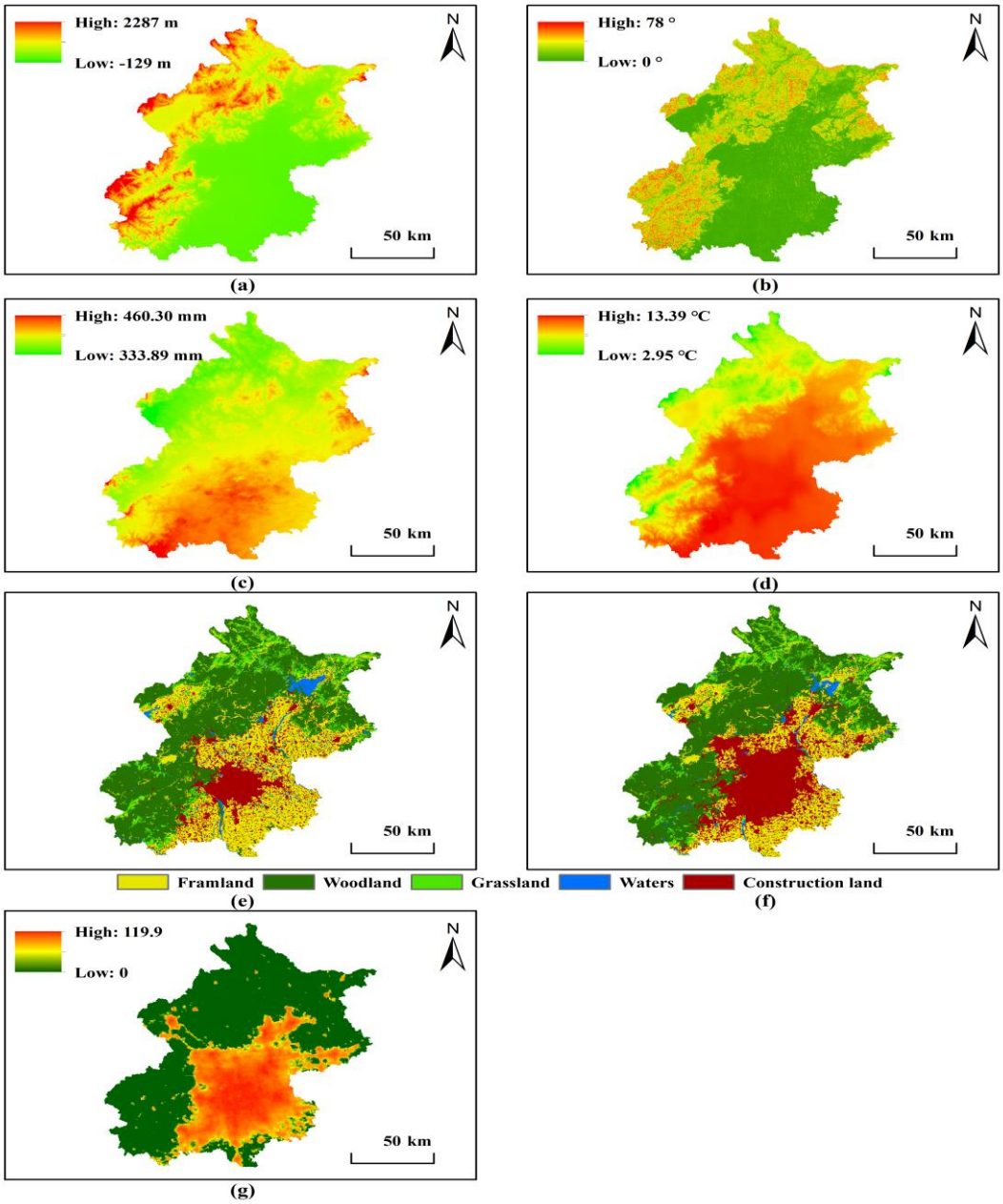

Figure 2. *Spatial distribution of altitude, slope, average annual precipitation, average annual temperature, land use and night time light in Beijing (a) The altitude, (b) slope, (c) average annual precipitation, (d) average annual temperature, (e) land use in 2000, (f) land use in 2015 and (g) night time light*

http://www.aloki.hu ● ISSN 1589 1623 (Print) ● ISSN 1785 0037 (Online)
DOI: http://dx.doi.org/10.15666/aeer/2006_48194834

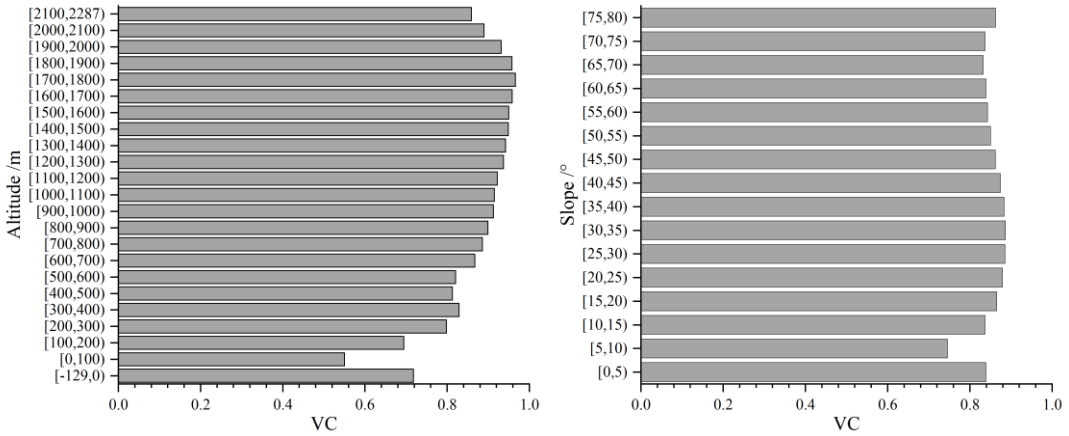

Figure 3. *The average VC at different altitudes or slopes*

The VC is highest (96.60%) in the altitude range of 1700 m to 1800 m and lowest (55.03%) in the altitude range of 0 m to 100 m. And the VC is highest (88.64%) in the slope range of 30° to 35° and lowest (74.56%) in the slope range of 5° to 10°. The dramatic decrease of VC in the altitude range of 0 to 100 m or the slope range of 5° to 10° may be caused by the high urbanization level of these areas. The construction land area within the range of 5 to 10° and the range of 0 to 100 m increased by 0.92 and 0.78 times during the period, respectively, and it was more than other ranges.

The effect of climate factors on VC

The average annual precipitation and temperature of the study area from 2000 to 2015 are shown in *Figure 2c* and *d*, respectively. The average annual precipitation ranged from 333.89 to 460.30 mm, with higher precipitation in the south and east than it in the west and north. And the average annual temperatures ranged from 2.95 to 13.39 ℃, with higher temperatures in the south and northeast than it in the southwest and northwest. The effects of precipitation and temperature on VC are shown in *Figure 4a* and *b*, respectively. Overall, there was a positive correlation between precipitation and VC in the study area, and the average correlation coefficient was 0.0433. In 42.52% of the study area, the precipitation was negatively correlated with VC, and it was mainly concentrated in the middle and south of the study area. Among them, 2.30% of the regions showed a significant negative correlation and the other 40.22% showed an insignificant negative correlation. In the other 57.48% of the study area, the precipitation was positively correlated with VC, it was mainly concentrated in the western and northern of the study area. Among them, 3.91% of the regions showed a significant positive correlation and the other 53.57% showed an insignificant positive correlation. For the whole study area, the increase of temperature also promoted the increase of VC, and the average correlation coefficient of them was 0.0512. In 41.26% of the study area, the temperature was negatively correlated with VC, and it was mainly concentrated in the northwest and southwest of the study area. Among them, 1.78% of the regions showed a significant negative correlation and the other 39.48% showed an insignificant negative correlation. In the other 58.74% of the study area, the temperature was positively correlated with VC, it was mainly concentrated in the northeast of the study area. Among them, 3.04% of the regions showed a significant positive correlation and the other 55.70% showed an insignificant positive correlation.

http://www.aloki.hu ● ISSN 1589 1623 (Print) ● ISSN 1785 0037 (Online)
DOI: http://dx.doi.org/10.15666/aeer/2006_48194834

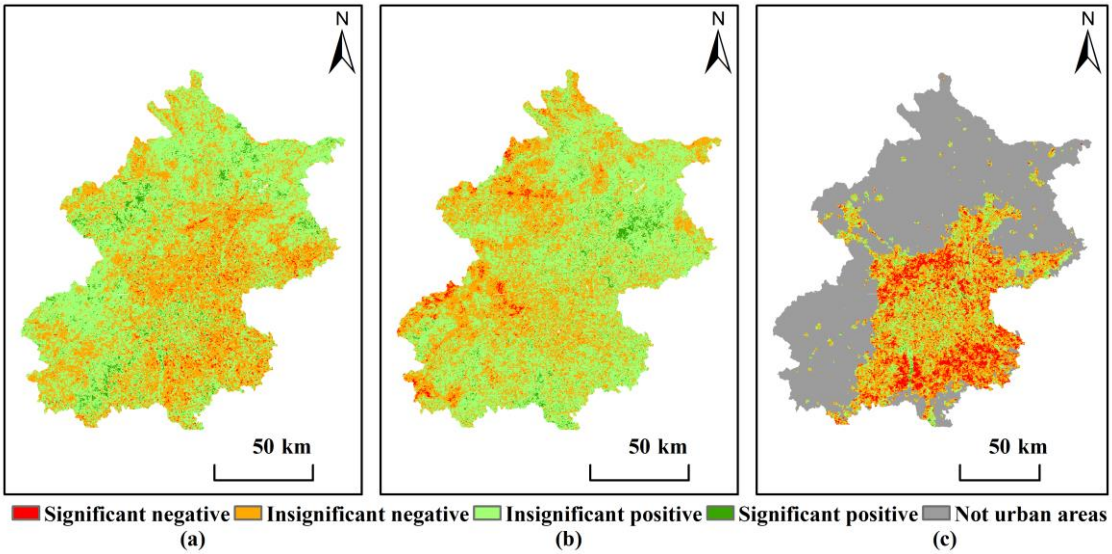

Figure 4. *The correlation between influence factors (precipitation (a), temperature (b) and urbanization (c)) and VC in Beijing*

The effect of urbanization level on VC

The average annual urbanization in the study area is shown in *Figure 2g*, it can be seen that the urban area occupied 40.92% of the study area and it was highly concentrated in the southeast. And the minimum urbanization is 0 and the maximum brightness is 119.919. The correlation between urbanization and VC is shown in *Figure 4c*, overall, they were negatively correlated with an average correlation coefficient of -0.1973. In the urban areas, 71.64% of the study area showed a negative correlation between the level of urbanization and VC, and it was mainly concentrated in the center of urban areas. Among them, 20.11% of the regions were significantly negatively correlated and the other 51.53% were insignificantly negatively correlated. Meanwhile, in the other 23.86% of the study area, they were positively correlated, and it was mainly concentrated in the periphery of urban areas. Among them, 1.77% of the regions were significantly positively correlated and the other 22.09% were insignificantly negatively correlated. As shown in *Figure 5*, the changing trend of VC was highest (0.57%/year) at urbanization level 5 and it was lowest (-1.51%/year) at urbanization level 8. Although there was a negative correlation between urbanization and VC, the changing trend of VC was not necessarily negatively correlated with the level of urbanization. The changing trend of VC basically increased from urbanization level 1 to 5, but decreases first and then increases at level 5-10.

The effect of land use on VC

The land use of the study area in 2000 and 2015 are shown in *Figure 2e* and *f*, respectively. According to statistical analysis, between 2000 and 2015, only the construction land had increased, and the increase rate of construction land was 118.9 km^2 per year. As the cost of urban development, the farmland, woodland, grassland and waters had decreased, and the decrease rate of them was 85.53, 8.87, 3.51 and 12.13 km^2 per year, respectively. As shown in *Table 1*, the farmland and waters mainly changed to construction land, the area was 1588 km^2 and 119 km^2, respectively,

http://www.aloki.hu ● ISSN 1589 1623 (Print) ● ISSN 1785 0037 (Online)
DOI: http://dx.doi.org/10.15666/aeer/2006_48194834

and for farmland, this proportion was as high as 50.90%. The woodland and construction land mainly changed to farmland, the area was 207 km^2 and 154 km^2, respectively. And the grassland mainly changed to the woodland (162 km^2).

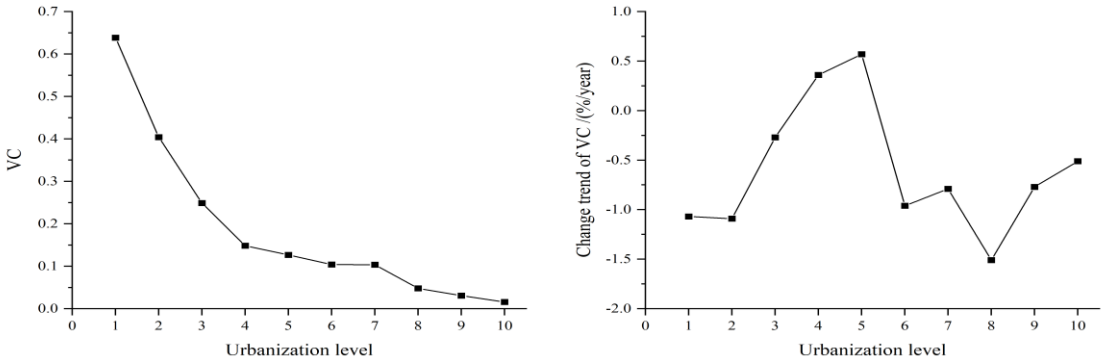

Figure 5. *The VC and its change trend under different urbanization levels. The night light brightness was divided into 10 levels on average to represent the urbanization levels, and the higher the night light brightness, the higher the urbanization level was*

Table 1. *Land use transfer matrix. The unit of transfer area is km^2, and the figures in brackets represent the change of VC*

		2000				
		Farmland	**Woodland**	**Grassland**	**Waters**	**Construction land**
2015	Farmland	3120 (-2.28%)	207 (-2.05%)	41 (2.74%)	109 (16.53%)	154 (-0.35%)
	Woodland	131 (-0.55%)	6970 (1.11%)	162 (3.47%)	20 (14.40%)	20 (3.45%)
	Grassland	42 (6.36%)	26 (5.32%)	1027 (5.54%)	9 (24.72%)	7 (4.76%)
	Waters	32 (-3.39%)	28 (3.81%)	7 (11.73%)	254 (14.15%)	8 (-3.13%)
	Construction land	1588 (-17.82%)	206 (-8.32%)	59 (-5.37%)	119 (-1.70%)	2057 (-4.18%)

When there was no change in land use, the VC of construction land and farmland decreased by 4.18% and 2.28% respectively, and the VC of woodland, grassland and waters increased by 1.11%, 5.54% and 14.15% respectively. When land use changed, the VC changed more drastically. The highest increase in VC was 24.72% when the waters changed to grassland, and the lowest increase in VC was 0.55% when the farmland changed to woodland. The highest decrease in VC was 17.82% when the farmland changed to construction land, and the lowest decrease in VC was 0.35% when the construction land changed to farmland.

Discussion

Based on NDVI, this paper estimated the vegetation coverage of Beijing from 2000 to 2015 by using the pixel dichotomy model. Purevdorj et al. (1998) once calculated the

http://www.aloki.hu ● ISSN 1589 1623 (Print) ● ISSN 1785 0037 (Online)
DOI: http://dx.doi.org/10.15666/aeer/2006_48194834

vegetation index according to the spectral reflectance of different vegetation cover, such as normalized difference, soil regulation, improved soil regulation and transformed soil regulated vegetation index (NDVI, SAVI, MSAVI and TSAVI), The second-order polynomial regression method is used to compare the relationship between various vegetation indexes and vegetation coverage. It is found that TSAVI and NDVI have the best estimation of vegetation coverage. The analysis of Xu et al. (2011) also shows that NDVI and RVI produce more accurate estimates of a wide range of vegetation cover. However, NDVI also has its disadvantages. First, it is very vulnerable to continuous cloud cover. At this time, its value will be lower than the normal value. Therefore, we use the maximum value synthesis method to obtain the maximum value of each pixel in a year, which is used to represent the NDVI at the time of the most vigorous vegetation growth. Second, NDVI is a nonlinear transformation, which enhances the low-value part of NDVI and suppresses the high-value part, resulting in easy saturation of NDVI value and reduced sensitivity to high-value density area.

Although night light data have been widely used in the study of the urban development process, there are few relevant applicable proofs. Zhang and Seto (2013) judge whether the urbanization of sample points has been correctly identified by comparing Google Earth and night light data. It is found that the accuracy rate of developed countries is higher than that of developing countries, and the overall accuracy rate of Oceania is the highest (93.3%), followed by North America, West South northern Europe, China and India (86.7%). In addition, a sound urban power infrastructure will also improve the identification accuracy. As the capital of China, there is no doubt about Beijing's high urbanization and perfect power infrastructure. Moreover, this paper does not make a quantitative analysis of Beijing's urbanization through night light data but uses continuous night light data to study the development process of urbanization, which can also improve the recognition of the trajectory of urbanization by night light data.

Vegetation coverage reflects the growth status of vegetation. This paper studied the influence of natural and human factors on this growth status. In terms of terrain, vegetation coverage increased first and then decreased with the increase in slope or altitude. Fu et al. (2011) found that the increase of slope led to more severe water and soil loss during rainfall. The experiment on eroded soil of Khan et al. (2013) in Samarbagh also proved that the higher the slope, the fewer soil nutrients. At the same time, Bangroo et al. (2017) found that the increase in altitude reduced the nutrients in the soil. However, most cities and towns in Beijing are on low altitudes and slopes. High human activities at the low altitude or slope impacted the vegetation growth. Thus, the altitude of -129-200 m and slope of 5-10° showed the lowest VC.

In terms of climate, precipitation and temperature both have a positive effect on the growth of vegetation, but this positive effect is minute. The areas where precipitation and temperature had significant positive effects on VC accounted for only 3.91% and 3.04% of the study area, respectively. Piao et al. (2014) believe that photosynthesis in the northern hemisphere is considered to have a positive response to the rise of temperature, but this effect is weakening with the adaptation of vegetation growth to climate warming. The increase in temperature can usually promote the photosynthetic rate of plants by increasing the activity of some enzymes and making plants grow better (Yamori et al., 2012). Vegetation needs water for photosynthesis. Appropriately increasing pre-precipitation can promote this process (Koyama and Kikuzawa, 2011; Slot and Winter, 2017), because the growth process of vegetation is actually a process

http://www.aloki.hu ● ISSN 1589 1623 (Print) ● ISSN 1785 0037 (Online)
DOI: http://dx.doi.org/10.15666/aeer/2006_48194834

of merging carbon dioxide and water into its own organic matter. However, different plant types have different demands on precipitation and temperature. When the precipitation or temperature exceeds a certain threshold, the growth of vegetation will be inhibited, which may also be the reason for the reduction of vegetation coverage in some areas. Moreover, excessive precipitation or temperature will form natural disasters, such as floods, debris flow, drought, etc. with the intensification of global climate instability, these disasters are more and more frequent, which is even more devastating for the growth of vegetation.

The impact of human activities on vegetation coverage is mainly reflected in urban development and land use change. It is generally believed that the impact of human activities on vegetation is often much greater than climate factors. This research found that the significant correlation area between urbanization and VC is larger than that between climate factors and VC, which proved this long-standing guess. This research found that the development of cities and towns has a huge negative impact on vegetation coverage, which is consistent with the research results of Zhao et al. (2021). At the same time, the changing trend of VC in high urbanization areas is not necessarily smaller than that in low urbanization areas, which may be caused by a series of reasons such as environmental protection awareness and available land area. In terms of land use, when farmland became construction land, the VC decreased the most (-17.82%), but why not woodland? It may be that the woodland in Beijing is mainly deciduous coniferous forest with low leaf density, while the farmland on the plain is planted with crops with high leaf density such as wheat all year round. And it is interesting to note that the vegetation coverage increased by 14.15% from 2000 to 2015 when the land use remained waters. The increase of VC in waters also proves that random sewage discharge to rivers in the process of urban development will lead to eutrophication of water bodies and an explosive increase of aquatic green plants such as algae.

Conclusion

By studying the changes of VC in Beijing from 2000 to 2015, this research found that the VC in the north and west of Beijing was higher than the VC in the south and east. The VC in Beijing decreased from 2000 to 2015, the average change trend of VC was -0.1534%/year. The VC decreased significantly in 19.33% of the study area and increased significantly in 13.78% of the study area. And the VC was low at an altitude range of -129~200 m and a slope range of 5°~10° where human activity was high. The VC was high in the altitude range of 1700 m to 1800 m or in the slope range of 30° to 35°. The increase of precipitation and temperature was conducive to the growth of vegetation. the positive correlation coefficients between precipitation, temperature and VC were 0.0433 and 0.0512, respectively. Increasing urbanization had a significant negative impact on VC, and the correlation coefficient was -0.1973. In urban areas of Beijing, 71.64% of the study area showed a negative correlation between the level of urbanization and VC, and this was more in the center of the urban areas than that in the periphery of urban areas. From 2000 to 2015, only the area of construction land in Beijing increased, while other land uses decreased. Changes in land use led to more drastic changes in vegetation coverage. The highest increase in VC was 24.72% when the waters was changed to grassland, and the highest decrease in VC was 17.82% when the grassland was changed to construction land.

http://www.aloki.hu ● ISSN 1589 1623 (Print) ● ISSN 1785 0037 (Online)
DOI: http://dx.doi.org/10.15666/aeer/2006_48194834

Acknowledgements. The study financial supported by the Special Program of Gaofen Satellites (grant NO. 21-Y30B02-9001-19/22-4). And we would like to thank the editors for their constructive suggestions and comments.

REFERENCES

[1] Bangroo, S. A., Najar, G. R., Rasool, A. (2017): Effect of altitude and aspect on soil organic carbon and nitrogen stocks in the Himalayan Mawer Forest Range. – CATENA 158: 63-68.

[2] Benjankar, R., Jorde, K., Yager, E. M., Egger, G., Goodwin, P., Glenn, N. F. (2012): The impact of river modification and dam operation on floodplain vegetation succession trends in the Kootenai River, USA. – Ecological Engineering 46: 88-97.

[3] Brandalise, M., Prandel, J., Quadros, F., Rovani, I., Malysz, M., Decian, V. (2019): Influence of urbanization on the dynamics of the urban vegetation coverage index (VCI) in Erechim (RS). – Floresta e Ambiente 26(2).

[4] Cai, S., Song, X., Hu, R., Guo, D. (2021): Ecosystem-dependent responses of vegetation coverage on the Tibetan Plateau to climate factors and their lag periods. – ISPRS International Journal of Geo-Information 10(6): 394.

[5] Fu, S., Liu, B., Liu, H., Xu, L. (2011): The effect of slope on interrill erosion at short slopes. – CATENA 84(1-2): 29-34.

[6] Gao, L., Wang, X., Johnson, B. A., Tian, Q., Wang, Y., Verrelst, J., Mu, X., Gu, X. (2020): Remote sensing algorithms for estimation of fractional vegetation cover using pure vegetation index values: a review. – ISPRS Journal of Photogrammetry and Remote Sensing 159: 364-377.

[7] Hao, J., Xu, G., Luo, L., Zhang, Z., Yang, H., Li, H. (2020): Quantifying the relative contribution of natural and human factors to vegetation coverage variation in coastal wetlands in China. – CATENA 188: 104429.

[8] Hu, T., Huang, X. (2019): A novel locally adaptive method for modeling the spatiotemporal dynamics of global electric power consumption based on DMSP-OLS nighttime stable light data. – Applied Energy 240: 778-792.

[9] Janeczko, E., Dąbrowski, R., Budnicka-Kosior, J., Woźnicka, M. (2019): Influence of Urbanization processes on the dynamics and scale of spatial transformations in the Mazowiecki Landscape Park. – Sustainability 11(11): 3007.

[10] Khan, F., Hayat, Z., Ahmad, W., Ramzan, M., Shah, Z., Sharif, M., Mian, I. A., Hanif, M. (2013): Effect of slope position on physico-chemical properties of eroded soil. – Soil Environ 32(1): 22-28.

[11] Koyama, K., Kikuzawa, K. (2011): Reduction of photosynthesis before midday depression occurred: leaf photosynthesis of Fagus crenata in a temperate forest in relation to canopy position and a number of days after rainfall. – Ecological Research 26(5): 999-1006.

[12] Leprieur, C., Verstraete, M. M., Pinty, B. (1994): Evaluation of the performance of various vegetation indices to retrieve vegetation cover from AVHRR data. – Remote Sensing Reviews 10(4): 265-284.

[13] Li, P., He, Z., He, D., Xue, D., Wang, Y., Cao, S. (2020): Fractional vegetation coverage response to climatic factors based on grey relational analysis during the 2000-2017 growing season in Sichuan Province, China. – International Journal of Remote Sensing 41(3): 1170-1190.

[14] Li, J., Wang, J., Zhang, J., Zhang, J., Kong, H. (2021): Dynamic changes of vegetation coverage in China-Myanmar economic corridor over the past 20 years. – International Journal of Applied Earth Observation and Geoinformation 102: 102378.

http://www.aloki.hu ● ISSN 1589 1623 (Print) ● ISSN 1785 0037 (Online)
DOI: http://dx.doi.org/10.15666/aeer/2006_48194834

[15] Liang, H., Guo, Z., Wu, J., Chen, Z. (2020): GDP spatialization in Ningbo City based on NPP/VIIRS night-time light and auxiliary data using random forest regression. – Advances in Space Research 65(1): 481-493.
[16] Liao, Q., Zhang, X., Ma, Q., Yao, Y., Yu, D. (2014): Spatiotemporal variation of fractional vegetation coverage and remote sensing monitoring in the eastern agricultural region of Qinghai Province. – Acta Ecologica Sinica 34(20): 5936-5943.
[17] Liu, H., Li, X., Mao, F., Zhang, M., Zhu, D., He, S., Huang, Z., Du, H. (2021): Spatiotemporal evolution of fractional vegetation cover and its response to climate change based on MODIS data in the subtropical region of China. – Remote Sensing 13(5): 913.
[18] Martínez, B., Gilabert, M. A., García-Haro, F. J., Faye, A., Meliá, J. (2011): Characterizing land condition variability in Ferlo, Senegal (2001-2009) using multi-temporal 1-km Apparent Green Cover (AGC) SPOT vegetation data. – Global and Planetary Change 76(3-4): 152-165.
[19] Pan, D., Song, Y., Dyck, M., Gao, X., Wu, P., Zhao, X. (2017): Effect of plant cover type on soil water budget and tree photosynthesis in jujube orchards. – Agricultural Water Management 184: 135-144.
[20] Piao, S., Nan, H., Huntingford, C., Ciais, P., Friedlingstein, P., Sitch, S., Peng, S., Ahlström, A., Canadell, J. G., Cong, N., Levis, S., Levy, P. E., Liu, L., Lomas, M. R., Mao, J., Myneni, R. B., Peylin, P., Poulter, B., Shi, X., … Chen, A. (2014): Evidence for a weakening relationship between interannual temperature variability and northern vegetation activity. – Nature Communications 5(1): 5018.
[21] Purevdorj, Ts., Tateishi, R., Ishiyama, T., Honda, Y. (1998): Relationships between percent vegetation cover and vegetation indices. – International Journal of Remote Sensing 19(18): 3519-3535.
[22] Rezaei, A., Gurdak, J. J. (2020): Large-scale climate variability controls on climate, vegetation coverage, lake and groundwater storage in the Lake Urmia watershed using SSA and wavelet analysis. – Science of The Total Environment 724: 138273.
[23] Sharifi, A. (2020): Remotely sensed vegetation indices for crop nutrition mapping. – Journal of the Science of Food and Agriculture 100(14): 5191-5196.
[24] Slot, M., Winter, K. (2017): In situ temperature response of photosynthesis of 42 tree and liana species in the canopy of two Panamanian lowland tropical forests with contrasting rainfall regimes. – New Phytologist 214(3): 1103-1117.
[25] Song, W., Mu, X., Ruan, G., Gao, Z., Li, L., Yan, G. (2017): Estimating fractional vegetation cover and the vegetation index of bare soil and highly dense vegetation with a physically based method. – International Journal of Applied Earth Observation and Geoinformation 58: 168-176.
[26] Wang, H., Yao, F., Zhu, H., Zhao, Y. (2020a): Spatiotemporal variation of vegetation coverage and its response to climate factors and human activities in arid and semi-arid areas: case study of the Otindag Sandy Land in China. – Sustainability 12(12): 5214.
[27] Wang, X., Zhang, S., Feng, L., Zhang, J., Deng, F. (2020b): Mapping maize cultivated area combining MODIS EVI Time series and the spatial variations of phenology over Huanghuaihai Plain. – Applied Sciences 10(8): 2667.
[28] Wang, M., Peng, J., Hu, Y., Du, Y., Qiu, S., Zhao, M. (2021): Scale consistency for investigating urbanization level, vegetation coverage, and their correlation. – Urban Forestry Urban Greening 59: 126998.
[29] Wu, D., Wu, H., Zhao, X., Zhou, T., Tang, B., Zhao, W., Jia, K. (2014): Evaluation of spatiotemporal variations of global fractional vegetation cover based on GIMMS NDVI data from 1982 to 2011. – Remote Sensing 6(5): 4217-4239.
[30] Xia, P., Yong, G., Ji, W. (2018): Response differences of MODIS-NDVI and MODIS-EVI to climate factors. – Journal of Resources and Ecology 9(6): 673.
[31] Xu, M., Yi, S., Ren, S., Ye, B., Zhou, Z. (2011): Study on estimation model of vegetation cover in the upstream regions of Shule River Basin based on hyperspectral. –

http://www.aloki.hu ● ISSN 1589 1623 (Print) ● ISSN 1785 0037 (Online)
DOI: http://dx.doi.org/10.15666/aeer/2006_48194834

International Conference on Remote Sensing, Environment and Transportation Engineering 4464-4471.

[32] Yamori, W., Masumoto, C., Fukayama, H., Makino, A. (2012): Rubisco activase is a key regulator of non-steady-state photosynthesis at any leaf temperature and, to a lesser extent, of steady-state photosynthesis at high temperature: regulation of photosynthesis by Rubisco activase. – The Plant Journal 71(6): 871-880.

[33] Yang, R., Li, X., Mao, D., Wang, Z., Tian, Y., Dong, Y. (2020): Examining fractional vegetation cover dynamics in response to climate from 1982 to 2015 in the Amur River basin for SDG 13. – Sustainability 12(14): 5866.

[34] Yuan, J., Xu, Y., Xiang, J., Wu, L., Wang, D. (2019): Spatiotemporal variation of vegetation coverage and its associated influence factor analysis in the Yangtze River Delta, eastern China. – Environmental Science and Pollution Research 26(32): 32866-32879.

[35] Zeng, X., Rao, P., DeFries, R. S., Hansen, M. C. (2003): Interannual variability and decadal trend of global fractional vegetation cover from 1982 to 2000. – Journal of Applied Meteorology 42(10): 1525-1530.

[36] Zhang, Q., Seto, K. (2013): Can night-time light data identify typologies of urbanization? A global assessment of successes and failures. – Remote Sensing 5(7): 3476-3494.

[37] Zhao, L., Wang, F., Dong, F., Xiao, C. (2021): Changes of vegetation coverage in Beijing in the background of urbanization based on the data from 2000 to 2019. – IOP Conference Series: Earth and Environmental Science 836(1): 012019.

[38] Zhou, Q., Zhao, X., Wu, D., Tang, R., Du, X., Wang, H., Zhao, J., Xu, P., Peng, Y. (2019): Impact of urbanization and climate on vegetation coverage in the Beijing–Tianjin–Hebei region of China. – Remote Sensing 11(20): 2452.

[39] Zribi, M., Le Hégarat-Mascle, S., Taconet, O., Ciarletti, V., Vidal-Madjar, D., Boussema, M. R. (2003): Derivation of wild vegetation cover density in semi-arid regions: ERS2/SAR evaluation. – International Journal of Remote Sensing 24(6): 1335-1352.

http://www.aloki.hu ● ISSN 1589 1623 (Print) ● ISSN 1785 0037 (Online)
DOI: http://dx.doi.org/10.15666/aeer/2006_48194834